# Guided ion beam studies of the reactions of $V_n^+$ ($n=2-13$) with $D_2$: Cluster–deuteride bond energies as a chemical probe of cluster electronic structure

Rohana Liyanage, J. Conceição, and P. B. Armentrout
*Department of Chemistry, University of Utah, Salt Lake City, Utah 84112*

(Received 10 September 2001; accepted 26 October 2001)

The kinetic energy dependencies of the reactions of $V_n^+$ ($n=2-13$) with $D_2$ are studied in a guided ion beam tandem mass spectrometer. Products observed are $V_nD^+$ for all clusters and $V_nD_2^+$ for $n=4-13$. All reactions are observed to exhibit thresholds, except for formation of $V_nD_2^+$ for $n=4,5,7,9,11-13$. The enhanced reactivity of the odd-sized clusters towards $D_2$ chemisorption is nicely correlated with the $D_0(V_n^+-V)$ bond energies. The odd-number clusters are less stable and more reactive, suggesting that they are open shell, whereas the even-number clusters, which are more stable and less reactive, appear to be closed shell. Threshold analyses of the endothermic reactions lead to $V_n^+-D$ binding energies ($n=1-13$), which reach values comparable to the bulk phase for larger clusters. The $V_n^+-D$ bond energies show odd–even oscillations anticorrelated with $D_0(V_n^+-V)$ for $n<5$, but roughly parallel with $D_0(V_n^+-V)$ for $n>5$. Magnitude differences in the two series of bond energies suggest that the metal–metal bonding has appreciable $3d-3d$ contributions. The variation in the $V_n^+-D$ bond energies with cluster size is explained using promotion energy arguments. © *2002 American Institute of Physics.* [DOI: 10.1063/1.1428342]

## I. INTRODUCTION

Metal clusters are a unique class of molecules that interpolate between two extremes, atomic and bulk phase. The chemical and physical properties of small metal clusters and the approach of these properties to the bulk phase values is a particularly interesting focus of cluster research.[1,2,3] In addition, it is useful to consider to what extent metal clusters can be used as a model of surfaces and their interactions with molecules in catalytic reactions. Catalytic reactions of CO and $H_2$ in Fischer–Tropsch (FT) processes[4] and $H_2$ and $N_2$ reactions in ammonia synthesis are two systems of considerable importance. Vanadium and other group 5 metals, niobium and tantalum, have a special affinity towards hydrogen, and can dissolve enormous amounts of hydrogen in the bulk.[5] Therefore, these metals play an important role in hydrogen storage technology. It is generally believed that the limiting step of hydrogen uptake into the bulk is the dissociation of molecular hydrogen on the surface.[5]

In addition to the potential practical importance of cluster research, clusters are ideal models for theoretical studies of surfaces and bulk phase properties. A number of theoretical studies in the literature have concerned the geometries, bonding, and magnetic properties of bare vanadium anion, neutral, and positive ion clusters.[6–11] The most recent work by Wu and Ray[11] uses all electron density functional theory with gradient corrections to the exchange correlation functions. These authors found bond energies for $V_2^+-V_9^+$ in reasonable agreement with values obtained in our laboratories by collision-induced dissociation (CID) experiments.[12] Theoretical work on the chemisorbtion of $H_2$ on metal surfaces and clusters in the past decade is extensive.[13–16] Dihydrogen chemisorbtion appears to be a particularly simple system that permits rigorous theoretical and experimental treatments.

Very little experimental information is available on the detailed electronic and geometric structures of transition metal clusters except for the smallest clusters.[17] Our group has studied CID of bare transition metal clusters [12,18–24] and their reactions with $D_2$, $O_2$, and $CH_4$,[25–29] as an ongoing effort to understand the reactivity, electronic structure, and geometry of transition metal clusters. These experimental studies have shown interesting variations with cluster size in the stability and reactivity of clusters. Bond dissociation energies (BDEs) of bare metal clusters, $D_0(M_n^+-M)$ for $n=2-20$ provide a quantitative assessment of cluster bonding, and some cases, insight into electronic structure. For example, odd–even oscillations observed in BDEs of small cationic vanadium clusters suggest the importance of $4s$ orbital participation in the metal–metal bonds. In previous studies of $Fe_n^+$ and $Cr_n^+$ reactions with $D_2$,[27,28] $M_n^+-D$ bond energies for larger clusters were found to be sufficiently strong that dissociative chemisorbtion of $D_2$ on these clusters should be exothermic. Yet, we observe clear barriers to these processes. Also, the odd-numbered chromium cluster cations bind weakly with D compared to even-sized clusters. These $Cr_n^+-D$ bond energies parallel those of $Cr_n^+-Cr$ indicating that interaction of $4s$ orbitals dominates both the metal–metal bonding and cluster-D bonding in chromium systems.

In the present study, we use guided ion beam tandem mass spectrometry to investigate the reactions of size-selected vanadium cluster cations (2–13 atoms) with $D_2$. Kinetic energy dependent cross sections for formation of $V_nD^+ + D$ and $V_nD_2^+$ product channels are determined. The former are interpreted to provide $V_n^+-D$ BDEs as a function of cluster size. Bond energy information for the larger clusters obtained here is favorably compared to bulk phase val-

 

ues. Cross sections for $V_nD_2^+$ formation are converted to kinetic energy dependent rate constants, $k(E)$, for chemisorption of $D_2$ on vanadium cation clusters. These are compared to rate constants obtained by Zakin *et al.*[30] and Dietrich *et al.*[31] for such processes at thermal energies.

## II. EXPERIMENT

The ion beam apparatus and experimental techniques used in this work have been described in detail elsewhere,[32] so only a brief description is given here. Vanadium cluster cations are formed by laser vaporization.[33] The output of an Oxford ACL 35 copper vapor laser operating at 8 kHz is tightly focused onto a continuously translating and rotating vanadium rod inside an aluminum source block. The optimum pulse energy for vanadium cluster ion production ranges between 3–4 mJ/pulse. The vaporized material is entrained in a continuous flow ($5-6\times10^3$ sccm) of He passing over the ablation surface. Frequent collisions and rapid mixing lead to the formation of thermalized clusters as they travel down a 2 mm diam$\times$63 mm long condensation tube. This seeded helium flow then undergoes a mild supersonic expansion in a field free region and is skimmed. Although direct measurements of the internal temperatures of the clusters are not possible, previous studies have indicated that the clusters are not internally excited and likely to be near room temperature.[18]

Positively charged ions are accelerated and injected into a 60° magnetic sector momentum analyzer. The mass selected ions are decelerated and focused into a rf octopole ion guide[34] that extends through a reaction cell. The octopole beam guide is biased with dc and rf voltages. The former allows accurate control of the translational energy of the incoming ions, whereas the latter establishes a radial potential that efficiently traps the parent and product ions that travel through the octopole. The pressure of $D_2$ neutral reactant gas (99.8% purity) in the reaction cell is kept relatively low to reduce the probability of multiple collisions with the ions. To test this, all studies were conducted at two pressures of $D_2$, ~0.2 and ~0.4 mTorr. The product and reactant ions drift to the end of the octopole, where they are extracted, and injected into a quadrupole mass filter for mass analysis. Ion intensities are measured with a Daly detector[35] coupled with standard pulse counting techniques. Reactant ion intensities ranged from $0.5-1.0\times10^6$ ions/s. Observed product intensities are converted to absolute reaction cross sections as discussed in detail elsewhere.[36] Absolute errors in the cross sections are on the order of $\pm30\%$.

Results for each reaction system were repeated several times to ensure their reproducibility. CID experiments with Xe were performed on all cluster ions to ensure their identity and the absence of any excessive internal excitation. In all instances, CID thresholds are consistent with those previously reported.[12] The absolute zero in the kinetic energy of the ions and their energy distributions (0.7–2.0 eV, gradually increasing with cluster size) were measured using the octopole as a retarding energy analyzer. The error associated with the zero of the absolute energy scale is 0.05 eV in the lab frame. Kinetic energies in the laboratory frame are converted to center-of-mass (CM) energies using the stationary target approximation, $E(\mathrm{CM})=E(\mathrm{lab})\ m/(m+M)$, where $m$ and $M$ are the masses of the neutral and ionic reactants, respectively. The data at the lowest energies are corrected for truncation of the ion beam energy distribution.[36]

Products observed in this work include $V_nD^+$ and $V_nD_2^+$ species. Accurate measurements of the intensities of these species depend on our ability to resolve and transport them efficiently to the detector. Resolving the high intensity $V_n^+$ reactant ions from the low intensity $V_nD^+$ product ions proved to be difficult even when the quadrupole mass analyzer was set to operate at high resolution. In principle, the resolution could be increased sufficiently to separate the parent and product ions, but as this limit is approached, the transmission of the ions is reduced to the extent that the experiments become impractical and inaccurate. Therefore the experiments are conducted using $D_2$ (to maximize the resolution) and by adjusting the resolution of the quadrupole mass filter to be as high as possible without reducing the product ion intensities. Mass overlap of product ions differing by two mass units is easily identified when the energy dependence of their cross sections differ, which is the case in this work.

## III. RESULTS

Vanadium cluster cations ranging in size from dimers to 13-mers were reacted with dideuterium as a function of kinetic energy over a range of thermal to about 10 eV. As shown in Fig. 1, only two types of products were observed as given in reactions (1) and (2),

$$V_n^+ + D_2 \rightarrow V_nD_2^+ \tag{1}$$

$$\rightarrow V_nD^+ + D. \tag{2}$$

Only reaction (2) is observed for clusters with $n=2$ and 3 atoms, whereas both reactions are observed for clusters with $n\geqslant4$ atoms. Reaction (2) is endothermic in all cases. Reaction (1) shows complex behavior as discussed in detail in the next section. It was verified that the magnitude of the cross sections for reactions (1) and (2) do not depend on the $D_2$ pressure, indicating that these cross sections correspond to single collisions between reactants. Also, we observed no products with fewer V atoms than the reactants, such as $V_{n-1}D^+$ or $V_{n-1}D_2^+$.

### A. Cross sections for $V_nD_2^+$ formation

The smallest cluster for which the $V_nD_2^+$ product is observed is the tetramer. However, the cross section for this product is small and noisy, making it difficult to ascertain definitively the energy dependence of this cross section. The pentamer shows much more substantial reactivity, as shown in Fig. 2. Here it can be seen that the cross section decreases monotonically with increasing energy, behavior that is characteristic of exothermic ion–molecule reactions. Although the data point density is low, the decline is roughly as $E^{-0.5}$ at the lowest energies, with a faster decline of about $E^{-1.8}$ above 0.1 eV. We believe that the probability of forming this $V_nD_2^+$ product is governed by the Langevin–Gioumousis–Stevenson (LGS) (Ref. 37) collision cross section as well as

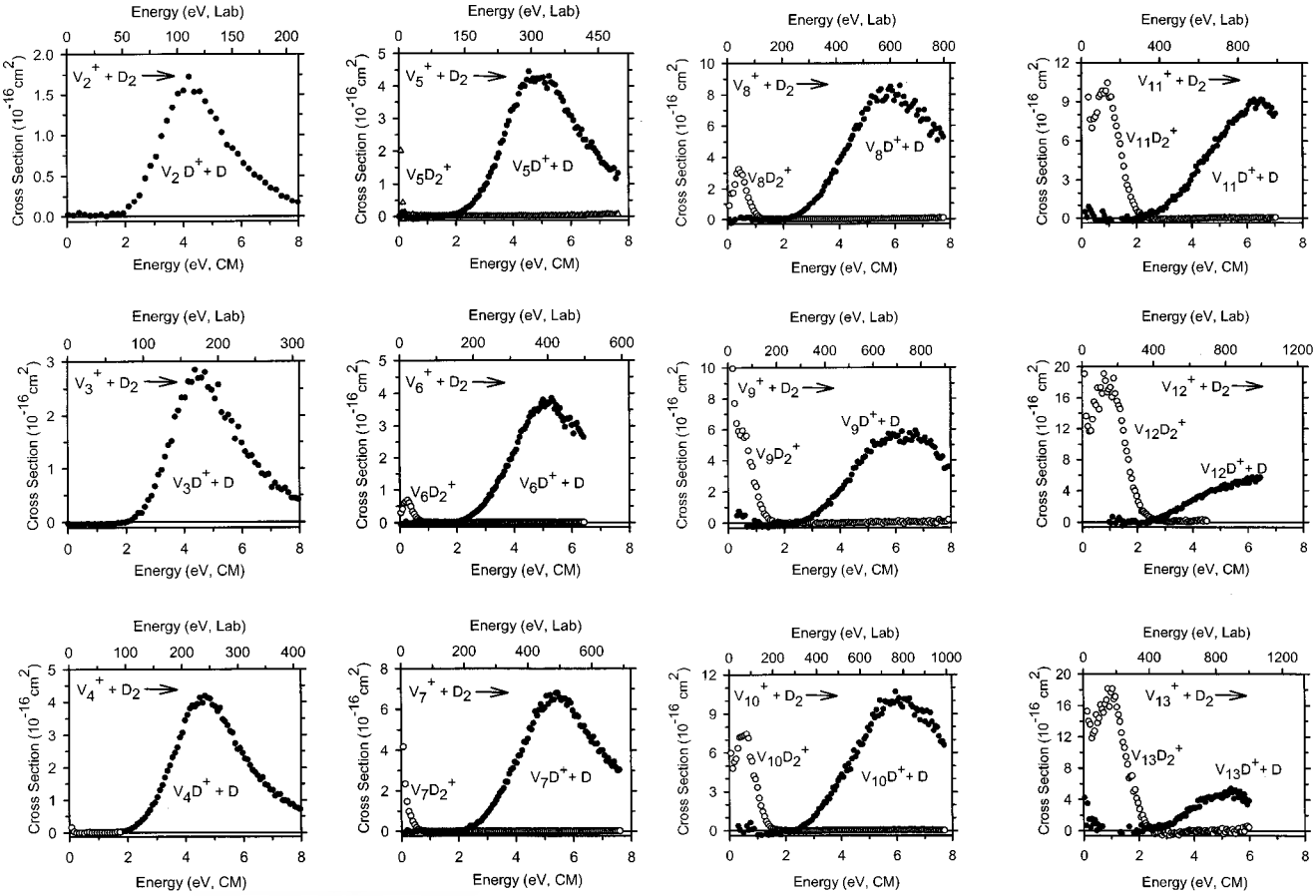


FIG. 1. Cross sections for reactions of $V_n^+$ ($n=2-13$) with $D_2$ as a function of collision energy in the center-of-mass (lower $x$-axis) and laboratory (upper $x$-axis) frames.

its lifetime, which decreases as the interaction energy increases. Observation of the $V_nD_2^+$ product is expected only if its lifetime exceeds or is on the order of the detection time window of our instrument, $\sim 10^{-4}$ s. One reason that we do not observe any $V_nD_2^+$ products for $n<4$ is probably because these cluster adducts dissociate more rapidly than this, even at low kinetic energies.

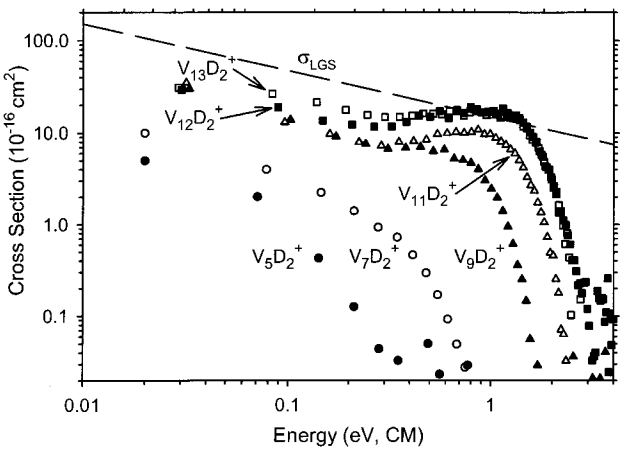


FIG. 2. Cross sections for reaction (1) plotted on a log scale for $n=5$, 7, 9, 11, 12, and 13 as a function of collision energy in the center-of-mass frame. The dashed line indicates the LGS model cross section (Ref. 37).

Similar to the pentamer, the heptamer shows a cross section that decreases roughly as $E^{-0.5}$ with increasing energy up to 0.3 eV, above which, it falls off rapidly as $E^{-1.9}$, Fig. 2. In contrast, $n=6$ and 8 clusters display $V_nD_2^+$ cross sections that increase in magnitude with increasing kinetic energy, behavior suggestive of endothermic reactions or barriers to reaction. The $n=9$, 11, 12, and 13 cluster cations were found to have cross sections exhibiting both exothermic and endothermic features, Fig. 2. The $n=10$ cluster is a transition point in that its cross section behaves primarily as if the reaction has a barrier, but may have a small exothermic tail at least one order of magnitude smaller than adjacent clusters. Overall, the magnitudes of the $V_nD_2^+$ cross sections increase as the cluster size increases, Figs. 1 and 2. Cross section magnitudes for $V_nD_2^+$ ($n=9,11-13$) are about half the LGS model prediction at the lowest energies, but the magnitudes of the cross sections decrease with increasing kinetic energy at similar rates, Fig. 2.

In all cases, the $V_nD_2^+$ product cross sections decline at elevated energies, typically reaching maxima at around 0.8–1.5 eV. This decline can be attributed to the overall reaction (3), as no other dissociation process is energetically accessible,

$$V_n^+ + D_2 \rightarrow V_nD_2^+ \rightarrow V_n^+ + D_2. \quad (3)$$

No energy is required for this overall process as the products

are the same as the initial reactants. The $V_nD_2^+$ product ion can conceivably have one of two forms: (1) a weakly-bound adduct held together by the ion-induced dipole attraction, i.e., a physisorbed state; or (2) a strongly-bound species where both deuterium atoms are chemically bonded to the cluster, i.e., a dissociatively chemisorbed state. In analogous systems,[27,28] we have previously argued that a weakly-bound adduct in which the $D_2$ molecule was intact should allow reaction (3) to be kinetically facile as well as being thermodynamically allowed at all collision energies. Consequently, it is difficult to understand how such a weakly-bound physisorbed species can survive our instrumental flight time of $10^{-4}$ s, unless it is collisionally stabilized by multiple collisions with $D_2$. Our pressure dependent studies verify that the $V_nD_2^+$ products are not the result of collisional stabilization. Further, the formation of a physisorbed adduct should not exhibit any barrier or endothermic threshold for any cluster size because the long-range ion-induced dipole potential between cluster ions and $D_2$ is attractive. Finally, the odd–even oscillations in reactivity are more difficult to explain for physisorbed species. Therefore, formation of $V_nD_2^+$ products does not behave as expected for physisorbtion processes in several regards.

In contrast, if the $V_nD_2^+$ clusters are dissociatively chemisorbed species, then reaction (3) requires that the two deuterium atoms come back together and pass through a tight transition state associated with cleaving the cluster-deuterium bonds and forming a $D_2$ bond. Such a process should be kinetically hindered, especially for larger clusters where the chemisorption energy can be dissipated throughout the cluster. This would explain the long lifetimes observed for $V_nD_2^+$ ($n>3$) products and why the magnitudes of the $V_nD_2^+$ cross sections increase for larger clusters. For the largest clusters where chemisorption is efficient, the cross sections are limited largely by the collision probability, such that the LGS model is roughly followed. The odd–even oscillations in these cross sections are also consistent with chemisorption, which should be sensitive to the electronic structure of the clusters, as discussed below. We therefore, conclude that the $V_nD_2^+$ products observed correspond to chemisorbed species.

### B. Cross sections for $V_nD^+$ formation

The formation of $V_nD^+$ in reaction (2) is observed to be endothermic for all clusters studied, Fig. 1. The kinetic energy dependencies of the cross sections are similar to those previously reported for $Fe_n^+$ and $Cr_n^+$ clusters reacting with $D_2$.[27,28] The cross sections exhibit apparent thresholds of $2.0\pm0.5$ eV for all clusters and reach maxima at 4–6 eV. The decline in the formation of $V_nD^+$ at elevated energies can be attributed to the overall reaction (4),

$$V_n^+ + D_2 \rightarrow V_nD^+ + D \rightarrow V_n^+ + 2D, \tag{4}$$

which can begin at $D_0(D_2)=4.56$ eV.[38] Smaller clusters exhibit an onset for this reaction close to its thermodynamic limit, 4.56 eV minus the internal energy of the cluster reactants. Figure 1 shows that the maxima in the cross sections increase as the cluster size increases. Larger clusters are able to accommodate more excess energy, so that the lifetime of the $V_nD^+$ product increases with increasing cluster size and eventually becomes larger than the $10^{-4}$ s time window available for dissociation in our experimental apparatus. At higher kinetic energies, the lifetime for dissociation becomes shorter than this time window and the dissociation process is again observed as declines in the $V_nD^+$ cross sections. Note that the observation of maxima in the $V_nD^+$ cross sections corresponding to reaction (4) is consistent with the failure to observe $V_nD^+$ products where $m<n$, i.e., $V_nD^+$ clusters preferentially dissociate by losing D rather than V atoms. Qualitatively, this result shows that $V_n^+-D$ bonds are weaker than $V_{n-1}^+-V$ bonds.

## IV. THRESHOLD ANALYSIS AND THERMOCHEMISTRY

The energy dependences of cross sections for endothermic processes can be modeled in the threshold region using Eq. (5),

$$\sigma(E)=\sigma_0\sum g_i(E+E_i-E_0)^N/E, \tag{5}$$

where $\sigma_0$ is an energy independent scaling parameter, $N$ is an adjustable parameter, $E$ is the relative kinetic energy, and $E_0$ is the threshold for the reaction at 0 K. The summation is over the rovibrational states of the clusters having energies $E_i$ and populations $g_i$, where $\Sigma g_i=1$. Vibrational frequencies for the bare metal clusters are obtained as outlined by Loh *et al.*,[32] who used a Debye model suggested by Jarrold and Bower.[39] Before comparison with the data, this model cross section is also convoluted with the kinetic energy distributions of the ion and neutral reactants.[36]

For metal clusters, it has been shown that lifetime effects become increasingly important as the size of the cluster increases.[18] This is because metal clusters have many low frequency vibrational modes such that the lifetime of the transient intermediate can exceed the experimental time available for reaction (approximately $10^{-4}$ s in our apparatus). Thus, an important component of the modeling of these reactions is to include the effect of the lifetime of the reaction, as estimated using statistical Rice–Ramsperger–Kassel–Marcus (RRKM) theory.[40-42] The use of RRKM theory is not entirely appropriate for species like transition metal clusters that have an appreciable density of electronic states. Unfortunately, more appropriate models are not yet available nor are there reliable means of accurately estimating the density of electronic states. Fortunately because both reactants and products share this high density of electronic states, errors associated with neglecting these states should largely cancel.

The means to incorporate lifetime effects in our modeling has been discussed in detail previously[43] and requires molecular constants for the energized molecule (EM) and transition state (TS) leading to the product of interest. For the primary reaction leading to $V_nD^+$, reaction (2), the energized molecule is the transiently formed $V_nD_2^+$ complex, which we assume has a $DV_nD^+$ structure, for reasons discussed above. For all species, the $3n-6$ vibrations associated with the metal cluster are assumed to equal those of the bare cluster

and are estimated using the Debye model.[39] For $DV_nD^+$, six additional frequencies are needed and are estimated as follows. We assume both deuterium atoms bind to two chemically equivalent bridging positions, although this assumption is not critical to the final results obtained. To obtain the asymmetric stretch frequency for $DV_n^+-D$, we first compare the asymmetric stretching frequencies determined experimentally for DFe–D (1200 $cm^{-1}$) (Ref. 44) and for DV–D (1085 $cm^{-1}$),[45] where the values are the average of frequencies measured in Kr and Ar matrices in both cases. This ratio (0.9) is used to scale frequencies previously estimated for $DFe_n^+-D$.[27] This gives values of 787 $cm^{-1}$ for the asymmetric stretch, 860 $cm^{-1}$ for the symmetric stretch, and 656 $cm^{-1}$ for the wag. Although this procedure may be over simplified, the magnitudes of the errors associated with these estimates of frequencies were evaluated by scaling all frequencies by ±25%, which produces differences in the thresholds that are less than 0.04 eV.

Formation of $V_nD^+ + D$ products from a $V_nD_2^+$ intermediate probably occurs via a loose transition state (LTS) located at the centrifugal barrier, which is treated variationally as described in detail elsewhere.[43] For ion–molecule reactions having no barriers in excess of the reaction endothermicity, this phase space limit (PSL) is a reasonable assumption.[40] For a PSL TS, the frequencies needed are simply those of the products, i.e., $V_nD^+ + D$. We also considered a tight transition state (TTS) model where we simply remove the frequency corresponding to the reaction coordinate, a cluster-D stretch. These two models should provide lower and upper limits to the dissociation rates of the $V_nD_2^+$ intermediates.

Our modeling of the $V_nD^+$ product cross sections includes energies above the point where the cross section declines as a result of product dissociation reaction (4). Including this region in our data analysis is advantageous because the more extensive energy range helps constrain the parameters in Eq. (5). This dissociation process can be modeled using simple statistical assumptions that are outlined elsewhere[46] and have been used successfully to describe the high energy behavior of the $V^+ + D_2 \rightarrow VD^+ + D$ reaction.[47] Briefly, Eq. (5) is multiplied by an energy dependent probability factor for product dissociation that depends on two adjustable parameters: $E_D$, the dissociation energy, and $p$, an empirical fitting parameter. Values of $p$ ranging from 1 to 5 were tested and a value of $p=3$ was found to best reproduce the data for most of the clusters. The same optimum value of $p$ was ascertained for the reactions of $Fe_n^+ + D_2$[27] and $Cr_n^+ + D_2$.[28]

### A. $V_n^+-D$ thresholds

Optimum values of the parameters of Eq. (5), $E_0$, $\sigma_0$, and $N$, used to reproduce the cross sections for the monodeuteride products are given in Table I. $V_nD^+$ product cross sections are modeled using both loose [phase space limit (PSL)] and tight transition states, as described above. A representative fit of data for the monodeuteride product ions is shown in Fig. 3. Thresholds measured in these experiments can be used to derive bond energies of $V_n^+-D$ by assuming there are no barriers to reaction (2) in excess of the endothermicity. This assumption has proved to be valid for many ion–molecule reactions because the long-range ion-induced dipole interactions between ions and polarizable neutrals are attractive. Exceptions often involve restrictions in spin or orbital angular momentum.[48] Unfortunately, conservation of such quantities cannot be examined for the present systems because detailed information concerning the electronic states of both reactants and products are not available. However, transition metal clusters have a dense manifold of electronic

TABLE I. Summary of parameters used in Eq. (5) for the analysis of $V_nD^+$ cross sections.[a]

| $n$ | $\sigma_0$[b] | $N$[b] | $E_0$ (TTS)[c] eV | $E_0$ (PSL)[d] eV | $D_0$ ($V_n^+-D$)[e] eV |
|---|---|---|---|---|---|
| 1 | | | | | 2.10 (0.06)[f] |
| 2 | 3.0 (1.0) | 1.2 (0.3) | 2.28 (0.16) | 2.32 (0.16) | 2.26 (0.18) |
| 3 | 6.0 (1.5) | 1.3 (0.3) | 2.65 (0.14) | 2.74 (0.14) | 1.86 (0.19) |
| 4 | 6.4 (2.0) | 1.6 (0.4) | 2.37 (0.18) | 2.51 (0.18) | 2.12 (0.25) |
| 5 | 4.4 (1.0) | 1.9 (0.3) | 2.11 (0.09) | 2.32 (0.09) | 2.34 (0.31) |
| 6 | 2.8 (1.5) | 2.3 (0.5) | 1.88 (0.18) | 2.15 (0.18) | 2.54 (0.32) |
| 7 | 5.2 (1.5) | 2.0 (0.2) | 1.80 (0.07) | 2.07 (0.07) | 2.63 (0.21) |
| 8 | 8.8 (2.5) | 1.8 (0.4) | 2.02 (0.15) | 2.47 (0.15) | 2.32 (0.38) |
| 9 | 2.0 (0.5) | 2.3 (0.2) | 1.70 (0.10) | 1.95 (0.10) | 2.73 (0.23) |
| 10 | 9.8 (2.5) | 1.6 (0.3) | 1.96 (0.11) | 2.54 (0.11) | 2.31 (0.40) |
| 11 | 8.4 (2.0) | 1.5 (0.2) | 1.74 (0.05) | 2.29 (0.05) | 2.56 (0.33) |
| 12 | 3.4 (1.5) | 1.8 (0.3) | 1.48 (0.12) | 1.90 (0.12) | 2.87 (0.48) |
| 13 | 5.0 (3.0) | 2.0 (0.3) | 1.56 (0.24) | 2.03 (0.24) | 2.77 (0.48) |

[a]Uncertainties in parentheses.
[b]Values for the PSL model. TTS parameters are similar.
[c]Tight transition state (TTS) model described in text.
[d]PSL model described in text.
[e]Average value derived from TTS and PSL thresholds according to Eq. (6).
[f]Value from Ref. 47.

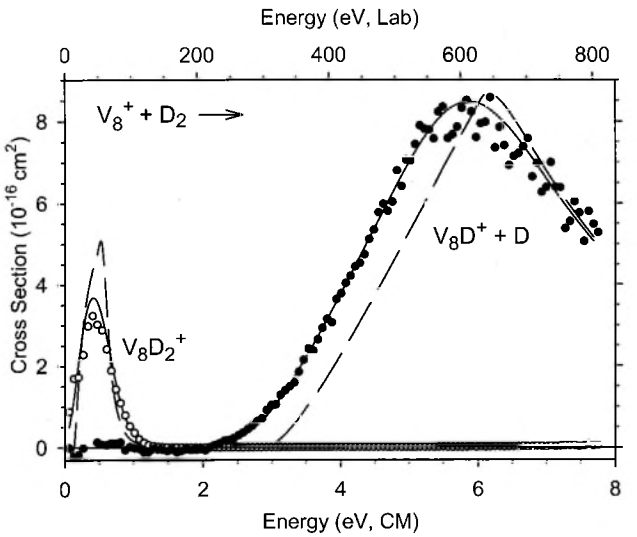


FIG. 3. Cross sections for reaction of $V_8^+$ with $D_2$ as a function of collision energy in the center-of-mass (lower $x$-axis) and laboratory (upper $x$-axis) frames. The dashed lines show the model of Eq. (5) with optimized parameters from Tables I and II along with a model for product dissociation. For the $V_8D_2^+$ product, no internal energy or RRKM lifetime effects were included, as described in the text, and the onset for dissociation was arbitrarily set to 0.9 eV to best reproduce the data. For the $V_8D^+ + D$ product channel, the analysis shown includes both internal energy and RRKM lifetime effects and the onset for product dissociation was set to 4.56 eV, the D–D bond dissociation energy. The solid lines show the models after convolution over the neutral and ion kinetic energy distributions.

TABLE II. Summary of parameters used in Eq. (5) for the analysis of $V_nD_2^+$ cross sections[a] and thermal rate constants for reaction (1).

| $n$ | $\sigma_0$[b] | $E_0$ (incl $E_i$) eV | $E_0$ (excl $E_i$) eV | $D_0$ ($DV_n^+-D$)[d] eV | $k\times10^{-9}$ ($cm^3\,s^{-1}$)[e] |
|---|---|---|---|---|---|
| 4 | ··· | <0 | <0 | >2.22 (0.16) | 0.003 (0.002) |
| 5 | ··· | <0 | <0 | >2.22 (0.16) | 0.04 (0.012) |
| 6 | 1.0 (0.3) | 0.34 (0.05) | 0.08 (0.05) | 1.94 (0.26) | 0.002 (0.001) |
| 7 | ··· | <0 | <0 | >1.93 (0.27) | 0.10 (0.03) |
| 8 | 3.8 (0.8) | 0.47 (0.08) | 0.15 (0.08) | 2.09 (0.36) | 0.005 (0.002) |
| 9 | ··· | <0 | <0 | >1.83 (0.37) | 0.35 (0.11) |
| 10 | 9.0 (1.0) | 0.50 (0.06) | 0.20 (0.06) | 2.05 (0.32) | 0.04 (0.01) |
| 11 | ··· | <0 | <0 | >2.00 (0.24) | 0.40 (0.12) |
| | 7.0 (1.5) | 0.60 (0.08)[c] | 0.10 (0.08)[c] | 1.90 (0.25) | |
| 12 | ··· | <0 | <0 | >1.69 (0.28) | 0.35 (0.11) |
| | 20.0 (2.5) | 0.75 (0.09)[c] | 0.25 (0.09)[c] | 1.44 (0.29) | |
| 13 | ··· | <0 | <0 | >1.79 (0.56) | 0.52 (0.16) |
| | 8.0 (1.5) | 0.65 (0.07)[c] | 0.15 (0.07)[c] | 1.64 (0.56) | |

[a]Uncertainties in parentheses.
[b]$N$ is fixed to 1.0 during optimization.
[c]Analysis of endothermic feature after subtraction of the model for exothermic reactivity. In all cases, it is likely that the values are lower limits. See text.
[d]Bond energies derived from the thresholds that exclude the internal energy.
[e]Rate constants for reaction (1) measured here at thermal energies and single collision conditions.

states, such that interactions (such as spin–orbit mixing) among these surfaces should allow adiabatic pathways for product formation without barriers in the excess of the endothermicities for $V_nD^+$. Thus we assume the thresholds for reactions leading to the formation of $V_nD^+$ represent the adiabatic endothermicities.

Given the assumption that there are no barriers in excess of the endothermicities to the formation of $V_nD^+ + D$, the thresholds for reaction (2), $E_0(2)$, can be converted to $V_n^+-D$ bond energies according to Eq. (6),

$$D_0(V_n^+-D)=D_0(D_2)-E_0(2). \tag{6}$$

Because Eq. (5) explicitly accounts for the internal energy and translational energy distributions of the reactants, the thermochemistry derived corresponds to 0 K. Bond energies calculated in this manner are given in Table I as the average of values from PSL and TTS threshold modeling.

### B. $V_nD_2^+$ thresholds

Optimum values of the parameters of Eq. (5), $E_0$, $\sigma_0$, and $N$, used to reproduce the cross sections for the dideuteride products are given in Table II. In the analysis of $V_nD_2^+$ cross sections using Eq. (5), we do not include RRKM lifetime effects because kinetic shifts cannot occur in the formation of the $V_nD_2^+$ products, the transient intermediates formed in the collision between reactants. We analyzed the cross sections for $n=6$, 8, and 10, as well as the endothermic features in the cross sections for $n=11-13$, after subtracting a model of the exothermic reactivity in these systems (using a simple power law). Figure 3 shows a representative model of such data. Thresholds obtained both with and without including internal energies of the reactant cluster ions are provided. The justification for excluding the internal energy in analysis of the reactions relies on other work. Theoretical studies of the reaction of the $Ni_{13}$ cluster with $D_2$ showed that the rates of reaction are insensitive to the temperature of the cluster over the range of 0–300 K.[49] Similarly, experimental results showed that the sticking probabilities of $H_2$ on Ni(111) surfaces,[50] an activated dissociative chemisorption process, are independent of the surface temperature. Finally, excluding the internal energy yielded the most reasonable thermochemistry for the analogous products, $Fe_nD_2^+$, in our previous cluster hydrogenation study.[27]

Reactions of $V_n^+$ clusters to form $V_nD_2^+$ exhibit clear thresholds for $n=6$, 8, and 10 and exhibit exothermic cross sections for $n=5$, 7, 9, 11, 12, and 13, whereas the behavior for $n=4$ is unclear. If the thresholds for even-sized clusters correspond to the endothermicity for dissociative chemisorption, then the measured thresholds can be used to derive $D_0(DV_n^+-D)$ values using Eq. (7),

$$\begin{aligned} D_0(DV_n^+-D)&=D_0(D_2)-E_0(1)-D_0(V_n^+-D)\\ &=E_0(2)-E_0(1). \end{aligned} \tag{7}$$

The validity of this assumption is explored below.

## V. DISCUSSION

### A. $V_n^+-D$ bond energies

The thresholds derived from analyses of the $V_nD^+$ cross sections using Eq. (5), assuming both loose and tight transition states, are listed in Table I. The PSL loose transition state model provides useful upper limits to the threshold energies and the tight transition state model provides lower limits. Both sets of energies show the same odd–even oscillations. Relative to the TTS values, thresholds obtained using the PSL model are the same for $V_2^+$ and then gradually increase. They are an average of $0.31\pm0.18$ eV higher than the TTS values for $n=2-13$ and $0.50\pm0.07$ eV for $n\geqslant10$. Because we do not know the nature of the transition state definitely, we conservatively take our best values for the $V_n^+-D$ bond energies as those derived using Eq. (6) from the average of the TTS and PSL threshold energies. This parallels our

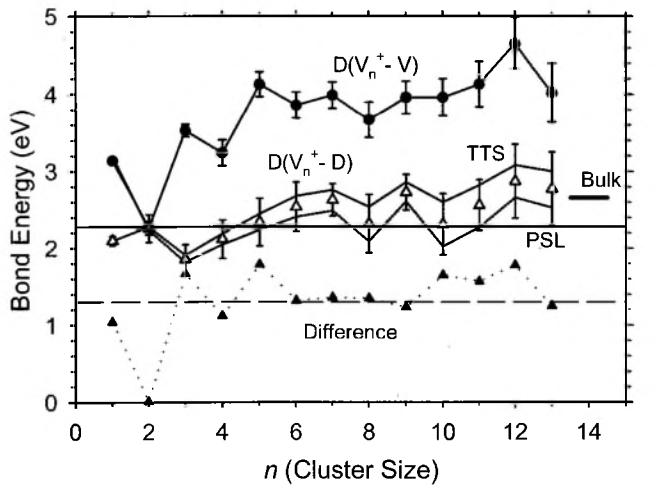


FIG. 4. $D_0(V_n^+-D)$ (△, Table I), $D_0(V_n^+-V)$ (●, Ref. 12), and their difference (▲) plotted as a function of cluster size, $n$. The horizontal dotted line indicates the average difference of $D_0(V_n^+-V)$ and $D_0(V_n^+-D)$ for $n=6-9$ and 13. The horizontal line at 2.28 eV indicates half the $D_0(D_2)$ bond energy. Two solid lines indicate the upper and lower limits to the $V_n^+-D$ bond energies obtained by analysis using PSL and TTS models. The small horizontal line indicates the bulk experimental binding energy of D to a V(100) surface from Ref. 5.

treatment for $Cr_n^+-D$ bond energies.[28] These $V_n^+-D$ bond energies are listed in Table I and shown in Fig. 4 along with uncertainties increased to reflect the span of values. It should be noted that the listed uncertainties reflect the absolute accuracy of each individual determination. Relative uncertainties, especially for adjacent cluster sizes, should be substantially smaller, on the order of 0.1 eV or less, because systematic errors in the interpretations cancel.

The accuracy of these values can be qualitatively assessed by consideration of the dissociative chemisorption of $D_2$ on the clusters. These chemisorbed $V_nD_2^+$ species are formed exothermically for odd clusters where $n\geq 5$, indicating that $D_0(DV_n^+-D)+D_0(V_n^+-D)>4.56\,\text{eV}=D_0(D_2)$. Assuming that the first and second cluster-deuterium bonds are roughly comparable, we should observe exothermic formation of $V_nD_2^+$ when $D_0(V_n^+-D)\geq D_0(D_2)/2=2.28\,\text{eV}$. This energy is indicated by a solid horizontal line in Fig. 4. As can be seen here, most bond energies obtained from both PSL and TTS models for odd clusters, $n\geq 5$, fall above this line. The only exception is the pentamer, where $D(V_5^+-D)$ obtained using the PSL model falls slightly below 2.28 eV, although even this value agrees within the uncertainty of the measurement. In reality, the $DV_n^+-D$ bond energy may oscillate out of phase with the $V_n^+-D$ bond energy for smaller clusters, such that $D(DV_n^+-D)\approx D(V_{n+1}^+-D)$. Thus a more accurate criterion for exothermic chemisorption might be that the sum of $D(V_{n+1}^+-D)$ and $D(V_n^+-D)$ should exceed $D_0(D_2)=4.56\,\text{eV}$. This alternate assumption does not lead to a change in the qualitative agreement for odd cluster sizes.

On the basis of the observed cross sections for $V_nD_2^+$, Fig. 1, chemisorption on even-sized clusters is either thermodynamically less favorable or kinetically less favorable than for odd-sized clusters. Given the weakness of the PSL bond energies for the $n=8$ and 10 clusters, it is conceivable that chemisorption on these clusters is endothermic, consistent with the failure to observe exothermic reactivity. However, the PSL bond energy for $V_6^+-D$ exceeds 2.28 eV, even though this cluster also exhibits a threshold for $V_6D_2^+$ formation. On the other hand, bond energies obtained from the TTS model all exceed 2.28 eV for $n\geq 5$, which would imply that even-sized clusters exhibit a barrier to exothermic chemisorption. Overall, these comparisons provide no definitive choice between the PSL and TTS models. Hence, our best estimation for $V_n^+-D$ bond energy remains those derived as the average of the two models, Table I.

### B. $D(DV_n^+-D)$ bond energies

If we use threshold analyses that do not consider the internal energy to be available to reaction, $D_0(DV_n^+-D)$ values obtained for $n=6$, 8, and 10 range from 1.9 to 2.1 eV. These values are lower than the analogous $D(V_n^+-D)$ bond energies by $0.4\pm0.2\,\text{eV}$ and lower than $D(V_{n+1}^+-D)$ by $0.6\pm0.1\,\text{eV}$. For larger clusters, it is hard to believe that a second D atom cannot find a binding site on the cluster comparable to the first D atom. A similar conclusion was reached previously in work done in our group[27] on $Fe_nD_2^+$ on the basis of studies by Liu *et al.*[51] These studies suggest comparable iron cluster-D atom BDEs up to the limit where the clusters are saturated with D atoms. Therefore, we conclude that the thresholds observed for reactions (1) with the even-sized clusters probably correspond to barriers to reaction. Therefore, the $D_0(DV_n^+-D)$ bond energies listed in Table II are considered accurate only as lower limits.

The binding energy of $H_2$ to $V_5^+$ has been measured by Dietrich *et al.* using collision-induced dissociation of $V_5H_2^+$ with Ar in an ion cyclotron resonance (ICR) mass spectrometer.[31] Dietrich *et al.* report a desorption energy of $2.4\pm0.3\,\text{eV}$, which indicates that $D(V_5^+-H)+D(HV_5^+-H)=6.9\pm0.3\,\text{eV}$. Combined with our value for $D(V_5^+-D)\approx D(V_5^+-H)$, Table I, this measurement would mean that $D(HV_5^+-H)\approx 4.5\pm0.4\,\text{eV}$ which is much larger than any of the bond energies in Tables I and II and than any known transition metal hydride bond energy.[52] Therefore, it seems likely that the desorption measurement either corresponds to a barrier or is subject to kinetic shifts.

### C. Comparison of $D(V_n^+-D)$ and $D(V_n^+-V)$

Figure 4 compares the cluster–deuteride bond energies with metal–metal bond energies for vanadium determined previously.[12] Except for $n=2$, $D_0(V_n^+-D)$ are much weaker than $D_0(V_n^+-V)$. Indeed, for $n\geq 5$, the metal–metal bonds average about $1.5\pm0.2\,\text{eV}$ ($58\pm11\%$) stronger than metal–deuterium bonds. It is known that first-row transition metal deuteride cations have bonds that mainly involve $4s-1s$ interactions,[47,52,53] and it seems likely that this should also be true of larger clusters. Therefore, the differences between the $V_n^+-D$ and $V_n^+-V$ bond energies suggest that $V_n^+-V$ bonding has strong contributions from both $4s-4s$ and $3d-3d$ interactions. This is distinct from the cases of $Fe_n^+$ and $Cr_n^+$, where $M_n^+-M$ and $M_n^+-D$ bond energies are more similar, and hence metal–metal bonding in the clusters is believed to be dominated by $4s-4s$ interactions.[27,28]

The pattern in the $V_n^+-V$ BDEs has previously been discussed in detail.[12] Calculations conducted subsequently have elucidated the geometrical structures but not the electronic structures of these species.[6–11] Briefly, the $V_2^+$ dimer cation is formed by binding ground state $V^+(^5D, 3d^4)$ with ground state $V(^4F, 4s^23d^3)$ to yield a $^2\Delta$ ground state with a $(4s\sigma_g)^2(3d\sigma_g)^2(3d\pi_u)^4(3d\delta_g)^1$ configuration. Walch and Bauschlicher[48] calculate that the trimer cation has a $^9A_2''$ ground state with a $(4sa_1')^2(3d\mathrm{MO})^{12}$ configuration (where $3d$MO indicates molecular orbitals originating from atomic $3d$ orbitals). Formation of this configuration therefore requires promotion of both $V_2^+$ and V to states each having single $4s$-like electrons. Thus, the promotion energy is sufficiently large that the $V_2^+-V$ BDE is the weakest of all vanadium cluster bond energies. Formation of $V_4^+$ having a $(4s\mathrm{MO})^4(3d\mathrm{MO})^{15}$ configuration, as previously postulated, can occur by combining ground state $V_3^+$ and ground state $V(^4F)$. For larger clusters up to $n=11$, the $V_n^+-V$ BDEs continue this even–odd oscillation with $n=$even bond energies being relatively weak compared to $n=$odd, which means that even-sized clusters are more stable than odd-sized clusters. This can be explained roughly in terms of sequential additions of $V(^6D, 4s^13d^4)$, the first excited state of V lying 0.26 eV above the $V(^4F, 4s^23d^3)$ ground state.[47] Clusters that have an even number of $4s$-like MOs (the even-sized clusters) bind $V(^6D)$ more weakly than those having an odd number of $4s$-like MOs (the odd-sized clusters). For larger clusters, geometrical effects have been suggested to become more important such that $V_{13}^+$ and $V_{15}^+$ are particularly stable clusters, and $V_{12}^+-V$ and $V_{14}^+-V$ bond energies are relatively strong.[12]

Comparison of the $V_n^+-D$ bond energies with the $V_n^+-V$ bond energies shows that the trends are roughly parallel for $n\geqslant 6$, Fig. 4. This is confirmation of our previous postulate that clusters in this size range can be understood largely by considering addition of $V(^6D, 4s^13d^4)$, electronically analogous to $D(^2S, 1s^1)$. As noted above, $3d-3d$ metal–metal interactions provide much stronger metal–metal bonds than metal–deuteride bonds, but apparently the variations in bonding are largely controlled by the $4s-4s$ and $4s-1s$ interactions. A more quantitative comparison of these bond energies finds that for most clusters, $n=6-9$ and 13, the $V_n^+-V$ bond energies are $1.3\pm0.1$ eV stronger than the $V_n^+-D$ bond energies, Fig. 4. The $n=4$ cluster shows a similar enhancement of $1.1\pm0.3$ eV. We take this difference to be a quantitative assessment of the $3d-3d$ bonding enhancement. For the other clusters, $n=5$ and 10–12, we speculate that there may be geometric contributions to the bond energy variations. In analogy with our observations for iron clusters,[27] this suggestion relies on the strong possibility that $V_6^+$ (octahedron) and $V_{13}^+$ (icosahedral or octahedral with fcc or bcc packing) can have highly symmetric geometrical structures compared to neighboring clusters. Substitution of D for V in such clusters breaks the symmetry, changing the molecular orbital ordering, thereby leading to less strongly bound systems. The $n=3$ cluster also shows a strong enhancement, which could indicate the stability of a tetrahedral $V_4^+$ cluster as calculated by Wu and Ray.[11]

In contrast to the larger clusters, smaller clusters, $n=1-4$, of vanadium show antiparallel $V_n^+-D$ and $V_n^+-V$ bond energies. For the monomer, this is straightforward to understand. As noted above, $V^+(^5D, 3d^4)$ can form a good $4s-4s$ covalent bond with $V(^4F, 4s^23d^3)$ because the vanadium atom can donate two $4s$ electrons. In contrast, formation of $VD^+(^4\Delta)$, which has a $(4s-1s\sigma)^2(3d\pi)^2(3d\delta)^1$ ground state configuration,[47] requires that $V^+$ be promoted to a $4s^13d^3$ configuration, which requires 0.7 eV including loss of the $s-d$ exchange energy.[53,52] Hence, $V^+-D$ is much weaker than $V^+-V$. When binding D to $V_2^+$, we note that there is a singly occupied $3d\delta_g$ orbital that could make a bond with a D $(1s^1)$ atom without any costly promotion. Alternatively, if bonding of D to a $4s$-like cluster orbital is needed, the relatively strong $V_2^+-D$ bond energy suggests that promotion of the $3d\delta_g$ electron to a $4s$-like orbital is not very costly, which may be because no exchange energy is lost in forming such a covalent bond, unlike for $VD^+$. For the trimer cation to bind to D using a $4s$-like orbital, it must promote an electron from the $3d$ orbitals to a $4se'$ orbital. This rationalizes a weak $V_3^+-D$ bond energy, Fig. 4, in contrast to the strong $V_3^+-V$ bond energy that can be formed by adding $V(^4F, 4s^23d^3)$, as noted above. This is directly analogous electronically to the situation for the monomer. For the tetramer, we imagine an analogous situation as the dimer exists in that the ground state, which likely has a closed-shell $(4s\mathrm{MO})^4$ configuration, must have a small promotion energy to a state with an available unpaired electron. The $n=5$ cluster appears to represent a transition between the regions where the $V_n^+-D$ and $V_n^+-D$ bond energies are antiparallel and parallel.

### D. Comparisons to bulk phase thermochemistry

According to studies on a V(100) surface, desorption of $D_2$ requires between 0.6 and 0.9 eV.[5,54] (Note this is much smaller than the value of $2.4\pm0.3$ eV measured by Dietrich *et al.* for $V_5H_2^+$.[31]) This indicates that the average binding energy of D to the V(100) surface is about $(4.56+0.75)/2 = 2.66\pm0.08$ eV. A theoretical bond energy for binding of a H atom to a vanadium surface is 3.1 eV, as obtained by Nørskov[55] using effective-medium theory.[56,57] This value is somewhat larger than the experimental value. As shown in Fig. 4, our $V_n^+-D$ bond energies for largest clusters reach values that are comparable to the experimental bulk phase value. Similar observations have been made for other cluster-deuteride bond energies, $Fe_n^+-D$ (Ref. 27) and $Cr_n^+-D$,[28] as well as several cluster–oxide bond energies, $Fe_n^+-O$,[25,26] $Cr_n^+-O$,[58,59] and $V_n^+-O$.[60]

### E. $D_2$ activation by $V_n^+$

Odd–even oscillations in the reactivity of vanadium cation clusters with $D_2$ and $H_2$ for the formation of $V_nD_2^+$ have been observed before by Zakin *et al.*[30] and Dietrich *et al.*[31] at thermal energies. In agreement with our observations, no reactivity is seen at thermal energies for the vanadium dimer and trimer cations. For larger clusters, these previous studies found that the even-sized clusters are much less reactive with both $H_2$ and $D_2$ than the odd-sized clusters. In general, reaction rates increase with cluster size and the odd–even oscil-

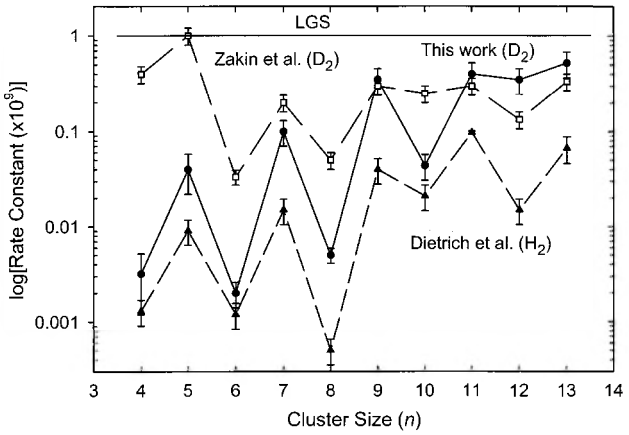


FIG. 5. Rate constants for reaction (1) at thermal energies plotted on a log scale. Solid circles and solid line indicate our experimental values, Table II; solid triangles and broken line indicate values from Ref. 31; and open squares and broken line indicate relative values obtained from Ref. 30, as normalized to the LGS value (horizontal line) at $n=5$.

lations in the reactivity begin to dampen for clusters $n>13$. These observations all agree well with our results. Similar odd–even oscillations in reactivity have been observed for reactions of neutral vanadium clusters with $D_2$,[61] and again the odd-sized clusters are more reactive.

Our cross sections can be converted to rate constants by using the expression, $k(\langle E\rangle)=\nu\sigma(E)$ where $\nu=(2E/\mu)^{1/2}$ and $\mu=mM/(m+M)$, the reduced mass of the reactants. The rate constants depend on the mean energy of the reactants, which includes the average thermal motion of the neutral, such that $\langle E\rangle=E+(3/2)\gamma k_B T$, where $\gamma=M/(m+M)$. Our rates for $D_2$ chemisorption at thermal energies are listed in Table II. Figure 5 compares our values with the absolute rates reported by Dietrich *et al.*[31] and the relative rates of Zakin *et al.*[30] normalized to the LGS rate at $n=5$. Reasonable agreement among the relative rates of all three studies is observed, especially with regard to the strong even–odd oscillations. Absolute values measured by Dietrich *et al.* are an average of about eight times smaller than our values, with our maximum rates being closer to the LGS value of $1.05\times10^{-9}$ cm$^3$ s$^{-1}$.[37] There is no obvious explanation for the deviations between the two sets of absolute values, which agree reasonably well considering that the experimental techniques employed are very different. The difference of $H_2$ vs $D_2$ reactants cannot provide an explanation as rates for $D_2$ should be about $2^{1/2}$ times (30%) slower than rates for $H_2$, a consequence of the difference in reduced masses of the reacting systems. It is possible that there are differences in the degree of thermalization (kinetic and internal) of the cluster ions in the two experiments that could lead to the observed differences.

## VI. SUMMARY

Reactions of $V_n^+$ ($n=2-13$) with $D_2$ are measured as a function of kinetic energy. The results are interpreted to yield thermal rates of chemisorption and $V_n^+$–D bond energies. For small clusters, $n<4$, dissociative chemisorption to form $V_nD_2^+$ products is probably endothermic, as suggested by $D(V_n^+-D)$ bond energies less than $D(D_2)/2=2.28$ eV. Although these products could be formed at elevated energies, apparently they dissociate back to reactants readily such that their lifetime is too short to observe. For odd-sized clusters larger than four atoms and even-sized clusters larger than eight atoms, chemisorption is observed to be exothermic, an observation consistent with the $V_n^+$–D bond energies. The larger size of these clusters presumably allows a sufficiently long lifetime of these $V_nD_2^+$ intermediates. The transition to efficient chemisorption is illustrated by the even-sized clusters $n=6$ and 8. These processes exhibit a barrier, which could be because the reaction is endothermic or because there is an activation barrier to chemisorption for these clusters.

Variations in the $V_n^+$–D BDEs can be rationalized using $4s$-type molecular orbitals on the clusters. Comparison between the $V_n^+$–D and previously determined[12] $V_n^+$–V bond energies[12] shows that the BDEs of D to $V_n^+$, which are presumably governed mainly by $4s-1s$ orbital interactions, are generally weaker than the binding of V to $V_n^+$, which must have strong contributions from both $4s-4s$ and $3d-3d$ interactions. Variations in the differences between $V_n^+$–V and $V_n^+$–D bond energies show that the $V_4^+$, $V_6^+$, and $V_{13}^+$ clusters are more stable than their neighbors, suggesting these clusters probably have highly symmetric geometric structures. For the largest clusters examined, we find that the $V_n^+$D bond energies reach relatively constant values that correspond well with values determined for binding D atoms to a V(100) surface.[5,54] This correspondence suggests that adsorbate binding is a local phenomenon that translates well from clusters to bulk surfaces.

## ACKNOWLEDGMENT

This work is supported by the Chemical Sciences, Geosciences, and Biosciences Division, Office of Basic Energy Sciences, Office of Science, U. S. Department of Energy.

[1] A. Kaldor, D. M. Cox, and R. M. Zakin, Adv. Chem. Phys. **70**, 211 (1988).
[2] D. M. Cox, K. C. Reichmann, D. J. Trevor, and A. Kaldor, J. Chem. Phys. **88**, 111 (1988).
[3] W. Weltner and R. Van Zee, Annu. Rev. Phys. Chem. **35**, 291 (1984).
[4] G. P. Van der Laan and A. A. C. M. Beenackers, Ind. Eng. Chem. Res. **38**, 1277 (1999).
[5] G. Krenn, C. Eibl, W. Mauritsch, E. L. D. Hebenstreit, P. Varga, and A. Winkler, Surf. Sci. **445**, 343 (2000).
[6] D. R. Salahub and R. P. Messmer, Surf. Sci. **106**, 415 (1981).
[7] F. Liu, S. N. Khanna, and P. Jena, Phys. Rev. B **43**, 8179 (1991).
[8] H. Dreysse, J. Doranates-Davila, A. Vega, L. C. Balbas, S. Bouarab, H. Nait-Laziz, and C. Demeangeat, J. Appl. Phys. **73**, 6207 (1993).
[9] K. Lee and J. Callaway, Phys. Rev. B **48**, 15358 (1993).
[10] H. Grönbeck and A. Rosen, J. Chem. Phys. **107**, 10620 (1997).
[11] X. Wu and A. K. Ray, J. Chem. Phys. **110**, 2437 (1999).
[12] C. X. Su, D. A. Hales, and P. B. Armentrout, J. Chem. Phys. **99**, 6613 (1993).
[13] I. Panas, P. Siegbahn, and U. Wahlgreen, Chem. Phys. **112**, 325 (1987).
[14] J. Harris and S. Anderson, Phys. Rev. Lett. **55**, 1583 (1985).
[15] D. J. Klinke II and L. J. Broadblet, Surf. Sci. **429**, 169 (1999).
[16] G. Blyholder, J. Head, and F. Ruette, Surf. Sci. **131**, 403 (1983).
[17] M. D. Morse, Chem. Rev. **86**, 1049 (1986).
[18] L. Lian, C. X. Su, and P. B. Armentrout, J. Chem. Phys. **97**, 4072 (1992).
[19] C. X. Su, D. A. Hales, and P. B. Armentrout, Chem. Phys. Lett. **201**, 199 (1993).
[20] C. X. Su and P. B. Armentrout, J. Chem. Phys. **99**, 6506 (1993).
[21] L. Lian, C. X. Su, and P. B. Armentrout, J. Chem. Phys. **97**, 4072 (1992).

[22] D. A. Hales, C. X. Su, and P. B. Armentrout, J. Chem. Phys. **100**, 1049 (1994).
[23] L. Lian, C. X. Su, and P. B. Armentrout, J. Chem. Phys. **96**, 7542 (1992).
[24] D. A. Hales, L. Lian, and P. B. Armentrout, Int. J. Mass Spectrom. Ion Processes **102**, 269 (1990).
[25] J. B. Griffin and P. B. Armentrout, J. Chem. Phys. **106**, 4448 (1997).
[26] J. B. Griffin and P. B. Armentrout, J. Chem. Phys. **107**, 5345 (1997).
[27] J. Conceição, S. K. Loh, L. Lian, and P. B. Armentrout, J. Chem. Phys. **104**, 3976 (1996).
[28] J. Conceição, R. Liyānage, and P. B. Armentrout, Chem. Phys. **262**, 115 (2000).
[29] R. Liyanage, X.-G. Zhang, and P. B. Armentrout, J. Chem. Phys. **115**, 9747 (2001).
[30] M. R. Zakin, D. M. Cox, R. O. Brickman, and A. Kaldor, J. Phys. Chem. **93**, 6823 (1989).
[31] G. Dietrich, K. Dagupta, S. Kuznestsov, K. Lützenkirchen, L. Schweikard, and J. Ziegler, Int. J. Mass Spectrom. Ion Processes **157/158**, 319 (1996).
[32] S. K. Loh, D. A. Hales, L. Lian, and P. B. Armentrout, J. Chem. Phys. **90**, 5466 (1989).
[33] T. G. Deitz, M. A. Duncan, D. E. Powers, and R. E. Smalley, J. Chem. Phys. **74**, 6511 (1981).
[34] E. Teloy and D. Gerlich, Chem. Phys. **4**, 417 (1974); D. Gerlich, Adv. Chem. Phys. **82**, 1 (1992).
[35] N. R. Daly, Rev. Sci. Instrum. **31**, 264 (1959).
[36] K. M. Ervin and P. B. Armentrout, J. Chem. Phys. **83**, 166 (1985).
[37] G. Gioumousis and D. P. Stevenson, J. Chem. Phys. **29**, 292 (1958).
[38] H. Huber and G. Herzberg, *Constants of Diatomic Molecules* (Van Nostrand Reinhold, New York, 1979).
[39] M. F. Jarrold and J. E. Bower, J. Chem. Phys. **87**, 5728 (1987).
[40] R. G. Gilbert and S. C. Smith, *Theory of Unimolecular and Recombination Reactions* (Blackwell Scientific, Oxford, 1990).
[41] D. G. Truhlar, B. C. Garrett, and S. J. Klippenstein, J. Phys. Chem. **100**, 12771 (1996).
[42] K. A. Holbrook, M. J. Pilling, and S. H. Robertson, *Unimolecular Reactions*, 2nd ed. (Wiley, New York, 1996).
[43] M. T. Rodgers, K. M. Ervin, and P. B. Armentrout, J. Chem. Phys. **106**, 4499 (1997).
[44] R. L. Rubinovitz and E. R. Nixon, J. Phys. Chem. **90**, 1940 (1986).
[45] Z. L. Xiao, R. H. Hauge, and J. L. Margrave, J. Phys. Chem. **95**, 2696 (1991).
[46] M. E. Weber, J. L. Elkind, and P. B. Armentrout, J. Chem. Phys. **84**, 1521 (1986).
[47] J. L. Elking and P. B. Armentrout, J. Phys. Chem. **89**, 5626 (1985).
[48] S. P. Walch and C. W. Bauschlicher, Jr., J. Chem. Phys. **83**, 5735 (1985).
[49] J. Jellinek and Z. B. Guvenc, Z. Phys. D: At., Mol. Clusters **26**, 110 (1993); in *Physics and Chemistry of Finite Systems: From Clusters to Crystals*, edited by P. Jena, S. N. Khanna, and B. K. Rao (Kluwer, Boston, 1992), Vols. I and II, p. 1047; in *Mode Selective Chemistry*, edited by J. Jortner, R. D. Levine, and B. Ullman (Kluwer, Boston, 1991), p. 153.
[50] H. J. Robota, W. Vielhaber, M. C. Lin, J. Segner, and G. Ertl, Surf. Sci. **155**, 101 (1985).
[51] K. Liu, E. K. Parks, S. C. Richtsmeier, L. G. Pobo, and S. J. Riley, J. Chem. Phys. **83**, 2882 (1985).
[52] P. B. Armentrout and B. L. Kickel, in *Organometallic Ion Chemistry*, edited by B. S. Freiser (Kluwer, Dordrecht, 1996), pp. 1–45.
[53] J. L. Elkind and P. B. Armentrout, J. Phys. Chem. **91**, 2037 (1987).
[54] M. Beutl, J. Lesnik, E. Laundgren, C. Konvicka, P. Varga, and K. D. Rendulic, Surf. Sci. **447**, 245 (2000).
[55] J. K. Nørskov, Rep. Prog. Phys. **53**, 1253 (1990).
[56] K. W. Jacobsen, J. K. Nørskov, and M. J. Puska, Phys. Rev. B **35**, 7423 (1987).
[57] P. Nordlander, S. Holloway, and J. N. Nørskov, Surf. Sci. **136**, 59 (1984).
[58] J. B. Griffin and P. B. Armentrout, J. Chem. Phys. **108**, 8062 (1998).
[59] J. B. Griffin and P. B. Armentrout, J. Chem. Phys. **108**, 8075 (1998).
[60] J. Xu, M. T. Rodgers, J. B. Griffin, and P. B. Armentrout, J. Chem. Phys. **108**, 9339 (1998).
[61] Y. M. Hamrick and M. D. Morse, J. Phys. Chem. **93**, 6494 (1989).